Published in final edited form as:

J Am Chem Soc. 2020 April 29; 142(17): 7725–7731. doi:10.1021/jacs.0c01065.

Photoactivatable Glycolipid Probes for Identifying Mycolate–Protein Interactions in Live Mycobacteria

Herbert W. Kavunja,
Department of Chemistry and Biochemistry, Central Michigan University, Mount Pleasant, Michigan 48859, United States

Kyle J. Biegas,
Department of Chemistry and Biochemistry, Central Michigan University, Mount Pleasant, Michigan 48859, United States

Nicholas Banahene,
Department of Chemistry and Biochemistry, Central Michigan University, Mount Pleasant, Michigan 48859, United States

Jessica A. Stewart,
Department of Chemistry and Biochemistry, Central Michigan University, Mount Pleasant, Michigan 48859, United States

Brent F. Piligian,
Department of Chemistry and Biochemistry, Central Michigan University, Mount Pleasant, Michigan 48859, United States

Jessica M. Groenevelt,
Department of Chemistry and Biochemistry, Central Michigan University, Mount Pleasant, Michigan 48859, United States

Caralyn E. Sein,
Department of Microbiology, University of Massachusetts, Amherst, Massachusetts 01003, United States

Yasu S. Morita,
Department of Microbiology and Molecular and Cellular Biology Graduate Program, University of Massachusetts, Amherst, Massachusetts 01003, United States

Michael Niederweis,
Department of Microbiology, University of Alabama at Birmingham, Birmingham, Alabama 35294, United States

Corresponding Author: Benjamin M. Swarts – Department of Chemistry and Biochemistry, Central Michigan University, Mount Pleasant, Michigan 48859, United States; ben.swarts@cmich.edu.

Supporting Information

The Supporting Information is available free of charge at https://pubs.acs.org/doi/10.1021/jacs.0c01065.
Supplementary figures and schemes, supplementary discussion, experimental methods, and ^{1}H and ^{13}C NMR spectra (PDF)
Proteomic data sets (XLSX)

Complete contact information is available at: https://pubs.acs.org/10.1021/jacs.0c01065

The authors declare no competing financial interest.

M. Sloan Siegrist,
Department of Microbiology and Molecular and Cellular Biology Graduate Program, University of Massachusetts, Amherst, Massachusetts 01003, United States

Benjamin M. Swarts
Department of Chemistry and Biochemistry, Central Michigan University, Mount Pleasant, Michigan 48859, United States;

Abstract

Mycobacteria have a distinctive glycolipid-rich outer membrane, the mycomembrane, which is a critical target for tuberculosis drug development. However, proteins that associate with the mycomembrane, or that are involved in its metabolism and host interactions, are not well-characterized. To facilitate the study of mycomembrane-related proteins, we developed photoactivatable trehalose monomycolate analogues that metabolically incorporate into the mycomembrane in live mycobacteria, enabling *in vivo* photo-cross-linking and click-chemistry-mediated analysis of mycolate-interacting proteins. When deployed in *Mycobacterium smegmatis* with quantitative proteomics, this strategy enriched over 100 proteins, including the mycomembrane porin (MspA), several proteins with known mycomembrane synthesis or remodeling functions (CmrA, MmpL3, Ag85, Tdmh), and numerous candidate mycolate-interacting proteins. Our approach is highly versatile, as it (i) enlists click chemistry for flexible protein functionalization; (ii) in principle can be applied to any mycobacterial species to identify endogenous bacterial proteins or host proteins that interact with mycolates; and (iii) can potentially be expanded to investigate protein interactions with other mycobacterial lipids. This tool is expected to help elucidate fundamental physiological and pathological processes related to the mycomembrane and may reveal novel diagnostic and therapeutic targets.

Mycobacteria are of enormous medical and biotechnological importance. The most prominent example is tuberculosis-causing *Mycobacterium tuberculosis* (*Mtb*), which kills 1.5 million people annually and exists in drug-resistant forms that are extremely challenging to treat.[1–4] Underlying the success of *Mtb* and related pathogens is a complex cell envelope containing a plasma membrane, peptidoglycan, arabinogalactan, and an outer membrane called the mycomembrane (Figure 1).[5–8] The mycomembrane consists of long, branched mycolic acids, which predominantly exist as mycolate esters linked to carbohydrates.[7–11] The mycomembrane is essential for survival due to its roles in cellular integrity and defense, nutrient acquisition, and cellular communication, including host–pathogen interactions.[9,10] Multiple drugs used to treat tuberculosis act on mycomembrane biosynthesis, highlighting why this membrane is a major focal point for mycobacteria research.[12]

Significant progress toward elucidating mycomembrane composition, biosynthesis, and function has been made, although much remains to be learned. Its major mycolate glycolipids, including trehalose monomycolate (TMM), trehalose dimycolate (TDM), and arabinogalactan mycolate (AGM), are synthesized as shown in Figure 1A. TMM is synthesized from trehalose in the cytoplasm via Pks13/CmrA[13] and then exported by MmpL3[14,15] and processed by Ag85 mycoloyltransferases[16–18] to generate TDM and AGM. However, the identities of many proteins involved in mycomembrane lipid transport,

remodeling, turnover, and host interactions have remained elusive. Furthermore, the proteomic composition of the mycomembrane is notoriously poorly defined.[19] Despite computational predictions that the *Mtb* genome may encode over 100 mycomembrane-associated proteins,[20–22] only a few have been identified and characterized across the *Mycobacterium* genus.[19,23–27] Most of these proteins exhibit channel activity and/or are important for nutrient influx, including the *Mycobacterium smegmatis* (*Msmeg*) porin (MspA),[23,28,29] *Mtb* CpnT,[24] and newly discovered *Mtb* PPE51.[30,31] The many as-yet unidentified mycomembrane proteins likely have other critical functions as well, including secretion/efflux processes, cell envelope biosynthesis and remodeling, and host–pathogen interactions.[19]

New tools are needed to accelerate the identification and functional characterization of mycomembrane-related proteins. Significant efforts have been made to enrich and identify mycomembrane-resident proteins,[27,32–36] mainly through subcellular fractionation and detergent extraction, but the resolution of cell envelope layers remains extremely challenging due to the massive peptidoglycan–arabinogalactan– mycolate covalent complex. Moreover, the lysis conditions, detergents, and centrifugation steps in these methods do not retain all of the protein–lipid interactions that occur *in vivo*, particularly weaker, transient interactions, which are frequently lost.[37] Such methods are also not designed to capture proteins that are not directly associated with the mycomembrane and thus miss an important subset of proteins involved in mycomembrane metabolism or host interactions. Finally, traditional methods are laborious and often incompatible with complex experimental contexts, *e.g.*, biofilm cultures or macrophage/animal infections. Recently, lipid-mimicking probes bearing photoactivatable and clickable groups have emerged as valuable tools for profiling *in vivo* lipid–protein interactions.[37–41] Here, we merged this photolabeling concept with our mycomembrane-targeting probes to develop the first tool for global analysis of *in vivo* mycolate–protein interactions, providing a powerful new approach to investigating mycomembrane-related proteins in their native state.

We reported that TMM analogues bearing functionalized mycolate-mimicking chains can metabolically incorporate into mycomembrane components via conserved, substrate-promiscuous Ag85 mycoloyltransferases.[42–44] By altering the linker, we controlled the incorporation mechanism and labeling target, with amide-linked N-AlkTMM-C7 exclusively labeling TDM and ester-linked O-AlkTMM-C7 labeling AGM and TDM (Scheme S1, Supporting Information (SI)).[42] Capitalizing on the TMM scaffold, we designed the two photoactivatable analogues N- and O-x-AlkTMM-C15 to enable mycomembrane proteomics (Figure 1B, SI Discussion). Both analogues possess the mycomembrane-targeting TMM moiety containing a lipophilic chain, which has a photoactivatable diazirine and a clickable alkyne. We envisioned that N- or O-x-AlkTMM-C15 would metabolically embed into glycolipids in live cells, placing the lipophilic chain in proximity to mycomembrane-related proteins. Upon UV photoactivation, the diazirine would photo-cross-link proteins, enabling click-mediated affinity enrichment from cell lysates and subsequent identification. In principle, this strategy enables capture and analysis of proteins that associate directly with the mycomembrane or that are involved in mycolate synthesis, transport, remodeling, turnover, or host interactions (SI Discussion).

The syntheses of both probes employed bifunctional fatty acid **1**,[39] which we conjugated to trehalose derivatives **2** and **3**[45–47] to produce N- and O-x-AlkTMM-C15 in two steps (Figure 2A). Using bovine serum albumin (BSA) as a model protein,[48] we confirmed that both probes possessed the requisite functionalities of (i) photo-cross-linking proteins when UV-irradiated and (ii) labeling and detecting the resulting cross-linked products via Cu-catalyzed azide–alkyne cycloaddition (CuAAC) (Figure 2B).

We tested whether N- and O-x-AlkTMM-C15 metabolically incorporated into the mycomembrane of live bacteria, focusing on the model organism *Msmeg*. Both TMM probes labeled *Msmeg* in a concentration- and time-dependent manner (Figure S1), whereas **1**, which lacks the trehalose targeting moiety, did not label the *Msmeg* surface (Figure S2). Partial growth inhibition for the probes was observed at 250 μM (Figure S3), indicating an optimal concentration of 25–100 μM. The probes were specific, as they efficiently labeled mycomembrane-containing *Msmeg* and *Corynebacterium glutamicum*, but not mycomembrane-deficient *Bacillus subtilis* or *Escherichia coli* (Figures 3A and S4). Consistent with the hypothesized incorporation routes (Scheme S1), N-x-AlkTMM-C15 labeling was entirely localized to the TDM-containing extractable lipids fraction and a new fluorescent lipid consistent with labeled TDM was observed, whereas O-x-AlkTMM-C15 labeling was detected in both the TDM- and AGM-containing fractions (Figures 3B and S5). The signal from both probes, and the peptidoglycan probe RADA[49] (positive control), was depleted upon spheroplast formation, which sheds the peptidoglycan–arabinogalactan–mycomembrane complex, leaving a spherical cell with the plasma membrane intact (Figure S6).[50,51] This result indicated that neither probe was detected in the plasma membrane. Incorporation of N-x-AlkTMM-C15 was reduced when *Msmeg* was co-incubated with an unlabeled TMM competitor or the Ag85 inhibitor ebselen[52] (Figures S7 and S8). Furthermore, an Ag85 partial knockout mutant[53] exhibited reduced labeling by N-x-AlkTMM-C15 compared to a control peptidoglycan probe[54] (Figure S9). Collectively, these data demonstrate that photoactivatable TMM analogues incorporate into the native mycomembrane as anticipated.

We next performed protein photo-cross-linking experiments in *Msmeg* using the TDM-targeting N-x-AlkTMM-C15 probe, which we prioritized primarily due to the complexities associated with O-x-AlkTMM-C15 labeling AGM (SI Discussion). N-x-AlkTMM-C15-treated live *Msmeg* was UV-irradiated, then lysates were collected, subjected to CuAAC with azido-488, and analyzed by SDS-PAGE. These experiments showed that proteins were labeled in a probe-, concentration-, and UV-dependent manner (Figure S10). *Msmeg* growth and metabolic activity were unaffected by UV irradiation (Figure S11), suggesting that UV-induced crosslinking in live cells occurred with minimal perturbation. To test whether N-x-AlkTMM-C15 photo-cross-linked our validation proteins, Ag85 and MspA, we enriched proteins and performed Western blot analysis. Probe-treated *Msmeg* was UV-irradiated, and then lysates were obtained and reacted with azido-TAMRA-PEG-biotin (AzTB) by CuAAC, delivering fluorescent and biotin tags to proteins for detection or enrichment. AzTB-treated lysates were analyzed by SDS-PAGE and Western blot prior to (input) and after (output) affinity capture on and elution from avidin beads. Proteins were effectively enriched only in the probe-treated, UV-irradiated (+probe+UV) samples (Figure 4A). Importantly, Ag85 and

MspA were detected in all input samples, while both were clearly enriched in the outputs of the +probe+UV samples (Figure 4B and SI Discussion). The plasma membrane-associated mannosyltransferase MptA (negative control) was not detected in the outputs (Figure S12). These results show that N-x-AlkTMM-C15 enables photo-cross-linking, affinity enrichment, and detection of mycolate-interacting proteins.

Finally, we used N-x-AlkTMM-C15 and label-free quantitative proteomics to identify mycolate–protein interactions in *Msmeg*, which was grown either for a shorter period to lower density (log phase) or an extended period to higher density (early stationary phase). In each of the two studies, LC−MS/MS analysis identified ~110 proteins that were significantly enriched by ≥4-fold in the +probe+UV group versus the probe−UV control, of which ~75 proteins were identified exclusively in the +probe+UV group (Figure 5 and Tables S1–S4). These identifications included multiple Ag85 isoforms and MspA, consistent with Western blot analysis (Figure 4B) and confirming that N-x-AlkTMM-C15 photo-cross-links mycolate-interacting proteins. Additional proteins with known mycolate-related functions were identified, including CmrA, which is involved in TMM synthesis,[55,56] and MmpL3, which is the TMM flippase.[14,15] We identified multiple relevant hydrolases, including TDM hydrolase (Tdmh), which is involved in stress-induced mycomembrane remodeling,[57–59] and two related proteins, MSMEG_1528 and MSMEG_0194 (55% and 41% sequence identity to Tdmh), which potentially represent novel mycomembrane-remodeling enzymes. Other notable hits include EccA1, whose absence in *Mycobacterium marinum* reduced mycolate synthesis by 40%,[60] and the extracellular proteins MTB12, MPT64, and HBHA, all of which have *Mtb* orthologs involved in host–pathogen interactions that are attractive diagnostic markers and/or vaccine candidates.[61–63] Indeed, most identified *Msmeg* proteins have *Mtb* orthologues, ~15–20% of which are essential for growth[64] and whose major predicted functions include cell wall/cell processes and uncharacterized hypothetical proteins (Tables S1 and S2; Figure S13). The differential protein profiles between our two studies, in terms of both protein identity and predicted functions (Figures 5C and S13), have interesting biological and experimental implications. The observed changes likely reflect a combination of growth-phase-dependent dynamic changes in mycolate–protein interactions and of improved detection of low-abundance interactions in higher-density cultures (SI Discussion). Finally, the successful identification of nearly all known trehalose mycolate-interacting proteins in *Msmeg* (see Figure 1A) provides high confidence in probe specificity and thus in the biological relevance of the proteins identified through our strategy.

Given the importance of the mycomembrane to mycobacterial physiology and tuberculosis drug development, it is perplexing that such wide gaps in knowledge still exist with respect to its proteomic composition and the identities of proteins involved in its metabolism and host interactions. To date, the extraordinary complexity of the mycobacterial cell envelope, and the lack of suitable tools to experimentally dissect it, have impeded progress toward elucidating the structures and functions of mycomembrane-related proteins. As a new approach to solving this problem, we reported the first probes for capturing lipid–protein interactions in live mycobacteria and demonstrated their ability to identify mycolate-interacting proteins with known functions spanning mycomembrane synthesis, transport, and remodeling. We generated and analyzed protein lists containing numerous candidate mycolate interactors, many with unknown function, which, along with the probes

themselves, are valuable for future research. Beyond expanding applications of N-x-AlkTMM-C15, we are further investigating O-x-AlkTMM-C15 and exploring a two-step approach using 6-TreAz[46] with our photoactivatable cyclooctynes.[48] Our tools' *in vivo* compatibility invites experimentation in diverse contexts (*e.g.*, spatiotemporal proteomics, biofilms, infection models), while their generality motivates application to other mycobacteria, most importantly *Mtb*, which is labeled by N- and O-x-AlkTMM-C15 (Figure S14). Our approach can also be extended to study endogenous or host protein interactions with other types of mycobacterial lipids, which are widely appreciated for their distinctive structures and biological importance. Ultimately, the ability to elucidate native-state lipid–protein interactions in mycobacteria will advance our understanding of mycobacterial physiology and pathogenesis, and may reveal new targets for the development of urgently needed tuberculosis vaccines, diagnostics, and drugs.

Supplementary Material

Refer to Web version on PubMed Central for supplementary material.

ACKNOWLEDGMENTS

This work was supported by NSF CAREER Award 1654408 (B.M.S.), Camille and Henry Dreyfus Foundation Henry Dreyfus Teacher–Scholar Award TH-17-034 (B.M.S.), NIH R21 AI144748 (Y.S.M. and M.S.S.), NIH R03 AI140259-01 (Y.S.M.), NIH DP2 AI138238 (M.S.S.), and NIH R01 AI121354 (M.N.). LC−MS/MS was performed at the Michigan State University Proteomics Facility by Douglas Whitten. We thank Dr. Kanna Palaniappan, Dr. Ben Luisi, and Dr. Amol Pohane for helpful discussions.

REFERENCES

(1). World Health Organization. Global Tuberculosis Report 2019, 10 17, 2019. https://www.who.int/tb/publications/global_report/en/.

(2). Glaziou P; Floyd K; Raviglione MC Global Epidemiology of Tuberculosis. Semin. Respir. Crit. Care Med 2018, 39, 271–285. [PubMed: 30071543]

(3). Dheda K; Gumbo T; Gandhi NR; Murray M; Theron G; Udwadia Z; Migliori GB; Warren R Global control of tuberculosis: from extensively drug-resistant to untreatable tuberculosis. Lancet Respir. Med 2014, 2, 321–338. [PubMed: 24717628]

(4). Kurz SG; Furin JJ; Bark CM Drug-Resistant Tuberculosis: Challenges and Progress. Infect. Dis. Clin. North Am 2016, 30, 509–522. [PubMed: 27208770]

(5). Brennan PJ Structure, function, and biogenesis of the cell wall of *Mycobacterium tuberculosis*. Tuberculosis 2003, 83, 91–97. [PubMed: 12758196]

(6). Angala SK; Belardinelli JM; Huc-Claustre E; Wheat WH; Jackson M The cell envelope glycoconjugates of *Mycobacterium tuberculosis*. Crit. Rev. Biochem. Mol. Biol 2014, 49, 361–399. [PubMed: 24915502]

(7). Hoffmann C; Leis A; Niederweis M; Plitzko JM; Engelhardt H Disclosure of the mycobacterial outer membrane: cryo-electron tomography and vitreous sections reveal the lipid bilayer structure. Proc. Natl. Acad. Sci. U. S. A 2008, 105, 3963–3967. [PubMed: 18316738]

(8). Zuber B; Chami M; Houssin C; Dubochet J; Griffiths G; Daffe M Direct visualization of the outer membrane of mycobacteria and corynebacteria in their native state. J. Bacteriol 2008, 190, 5672–5680. [PubMed: 18567661]

(9). Barry CE; Lee RE; Mdluli K; Sampson AE; Schroeder BG; Slayden RA; Yuan Y Mycolic acids: Structure, biosynthesis and physiological functions. Prog. Lipid Res 1998, 37, 143–179. [PubMed: 9829124]

(10). Marrakchi H; Lanéelle M-A; Daffé M Mycolic acids: structures, biosynthesis, and beyond. Chem. Biol 2014, 21, 67–85. [PubMed: 24374164]

(11). Sani M; Houben ENG; Geurtsen J; Pierson J; de Punder K; van Zon M; Wever B; Piersma SR; Jimenez CR; Daffe M; Appelmelk BJ; Bitter W; van der Wel N; Peters PJ Direct visualization by cryo-EM of the mycobacterial capsular layer: a labile structure containing ESX-1-secreted proteins. PLoS Pathog 2010, 6, No. e1000794. [PubMed: 20221442]

(12). North EJ; Jackson M; Lee RE New approaches to target the mycolic acid biosynthesis pathway for the development of tuberculosis therapeutics. Curr. Pharm. Des 2013, 20, 4357–4378.

(13). Gavalda S; Bardou F; Laval F; Bon C; Malaga W; Chalut C; Guilhot C; Mourey L; Daffé M; Quémard A The Polyketide Synthase Pks13 Catalyzes a Novel Mechanism of Lipid Transfer in Mycobacteria. Chem. Biol 2014, 21, 1660–1669. [PubMed: 25467124]

(14). Grzegorzewicz AE; Pham H; Gundi VAKB; Scherman MS; North EJ; Hess T; Jones V; Gruppo V; Born SEM; Korduláková J; Chavadi SS; Morisseau C; Lenaerts AJ; Lee RE; McNeil MR; Jackson M Inhibition of mycolic acid transport across the *Mycobacterium tuberculosis* plasma membrane. Nat. Chem. Biol 2012, 8, 334–341. [PubMed: 22344175]

(15). Xu Z; Meshcheryakov VA; Poce G; Chng S-S MmpL3 is the flippase for mycolic acids in mycobacteria. Proc. Natl. Acad. Sci. U.S. A 2017, 114, 7993–7998. [PubMed: 28698380]

(16). Sathyamoorthy N; Takayama K Purification and characterization of a novel mycolic acid exchange enzyme from *Mycobacterium smegmatis*. J. Biol. Chem 1987, 262, 13417–13423. [PubMed: 3654621]

(17). Belisle JT; Vissa VD; Sievert T; Takayama K; Brennan PJ; Besra GS Role of the major antigen of *Mycobacterium tuberculosis* in cell wall biogenesis. Science 1997, 276, 1420–1422. [PubMed: 9162010]

(18). Dautin N; de Sousa-d'Auria C; Constantinesco-Becker F; Labarre C; Oberto J; de la Sierra-Gallay IL; Dietrich C; Issa H; Houssin C; Bayan N Mycoloyltransferases: A large and major family of enzymes shaping the cell envelope of Corynebacteriales. Biochim. Biophys. Acta, Gen. Subj 2017, 1861, 3581–3592. [PubMed: 27345499]

(19). Niederweis M; Danilchanka O; Huff J; Hoffmann C; Engelhardt H Mycobacterial outer membranes: in search of proteins. Trends Microbiol 2010, 18, 109–116. [PubMed: 20060722]

(20). Pajon R; Yero D; Lage A; Llanes A; Borroto CJ Computational identification of beta-barrel outer-membrane proteins in *Mycobacterium tuberculosis* predicted proteomes as putative vaccine candidates. Tuberculosis 2006, 86, 290–302. [PubMed: 16542876]

(21). Song H; Sandie R; Wang Y; Andrade-Navarro MA; Niederweis M Identification of outer membrane proteins of *Mycobacterium tuberculosis*. Tuberculosis 2008, 88, 526–544. [PubMed: 18439872]

(22). Mah N; Perez-Iratxeta C; Andrade-Navarro MA Outer membrane pore protein prediction in mycobacteria using genomic comparison. Microbiology 2010, 156, 2506–2515. [PubMed: 20466765]

(23). Stahl C; Kubetzko S; Kaps I; Seeber S; Engelhardt H; Niederweis M MspA provides the main hydrophilic pathway through the cell wall of Mycobacterium smegmatis. Mol. Microbiol 2001, 40, 451–464. [PubMed: 11309127]

(24). Danilchanka O; Sun J; Pavlenok M; Maueröder C; Speer A; Siroy A; Marrero J; Trujillo C; Mayhew DL; Doornbos KS; Muñoz LE; Herrmann M; Ehrt S; Berens C; Niederweis M An outer membrane channel protein of *Mycobacterium tuberculosis* with exotoxin activity. Proc. Natl. Acad. Sci. U. S. A 2014, 111, 6750–6755. [PubMed: 24753609]

(25). Speer A; Rowland JL; Haeili M; Niederweis M; Wolschendorf F Porins increase copper susceptibility of *Mycobacterium tuberculosis*. J. Bacteriol 2013, 195, 5133–5140. [PubMed: 24013632]

(26). Speer A; Sun J; Danilchanka O; Meikle V; Rowland JL; Walter K; Buck BR; Pavlenok M; Hölscher C; Ehrt S; Niederweis M Surface hydrolysis of sphingomyelin by the outer membrane protein Rv0888 supports replication of *Mycobacterium tuberculosis* in macrophages. Mol. Microbiol 2015, 97, 881–897. [PubMed: 26036301]

(27). van der Woude AD; Mahendran KR; Ummels R; Piersma SR; Pham TV; Jiménez CR; de Punder K; van der Wel NN; Winterhalter M; Luirink J; Bitter W; Houben ENG Differential detergent extraction of Mycobacterium marinum cell envelope proteins identifies an extensively modified

threonine-rich outer membrane protein with channel activity. J. Bacteriol 2013, 195, 2050–2059. [PubMed: 23457249]

(28). Stephan J; Bender J; Wolschendorf F; Hoffmann C; Roth E; Mailander C; Engelhardt H; Niederweis M The growth rate of Mycobacterium smegmatis depends on sufficient porin-mediated influx of nutrients. Mol. Microbiol 2005, 58, 714–730. [PubMed: 16238622]

(29). Faller M; Niederweis M; Schulz GE The Structure of a Mycobacterial Outer-Membrane Channel. Science 2004, 303, 1189–1192. [PubMed: 14976314]

(30). Wang Q; Boshoff HIM; Harrison JR; Ray PC; Green SR; Wyatt PG; Barry CE PE/PPE proteins mediate nutrient transport across the outer membrane of *Mycobacterium tuberculosis*. Science 2020, 367, 1147–1151. [PubMed: 32139546]

(31). Korycka-Machala M; Pawelczyk J; Borowka P; Dziadek B; Brzostek A; Kawka M; Bekier A; Rykowski S; Olejniczak AB; Strapagiel D; Witczak Z; Dziadek J PPE51 Is Involved in the Uptake of Disaccharides by *Mycobacterium tuberculosis*. Cells 2020, 9, No. E603. [PubMed: 32138343]

(32). Rezwan M; Lanéelle MA; Sander P; Daffé M Breaking down the wall: Fractionation of mycobacteria. J. Microbiol. Methods 2007, 68, 32–39. [PubMed: 16839634]

(33). Marchand CH; Salmeron C; Bou Raad R; Méniche X; Chami M; Masi M; Blanot D; Daffé M; Tropis M; Huc E; Le Maréchal P; Decottignies P; Bayan N Biochemical Disclosure of the Mycolate Outer Membrane of Corynebacterium glutamicum. J. Bacteriol 2012, 194, 587–597. [PubMed: 22123248]

(34). Chiaradia L; Lefebvre C; Parra J; Marcoux J; Burlet-Schiltz O; Etienne G; Tropis M; Daffé M Dissecting the mycobacterial cell envelope and defining the composition of the native mycomembrane. Sci. Rep 2017, 7, 12807. [PubMed: 28993692]

(35). He Z; De Buck J Cell wall proteome analysis of Mycobacterium smegmatis strain MC2 155. BMC Microbiol 2010, 10, 121. [PubMed: 20412585]

(36). McNamara M; Tzeng SC; Maier C; Zhang L; Bermudez LE Surface proteome of "Mycobacterium avium subsp. hominissuis" during the early stages of macrophage infection. Infect. Immun 2012, 80, 1868–1880. [PubMed: 22392927]

(37). Peng T; Yuan X; Hang HC Turning the spotlight on protein-lipid interactions in cells. Curr. Opin. Chem. Biol 2014, 21, 144–153. [PubMed: 25129056]

(38). Gubbens J; Ruijter E; de Fays LEV; Damen JMA; de Kruijff B; Slijper M; Rijkers DTS; Liskamp RMJ; de Kroon AIPM Photocrosslinking and Click Chemistry Enable the Specific Detection of Proteins Interacting with Phospholipids at the Membrane Interface. Chem. Biol 2009, 16, 3–14. [PubMed: 19171301]

(39). Haberkant P; Raijmakers R; Wildwater M; Sachsenheimer T; Brügger B; Maeda K; Houweling M; Gavin A-C; Schultz C; van Meer G; Heck AJR; Holthuis JCM In Vivo Profiling and Visualization of Cellular Protein–Lipid Interactions Using Bifunctional Fatty Acids. Angew. Chem., Int. Ed 2013, 52, 4033–4038.

(40). Hulce JJ; Cognetta AB; Niphakis MJ; Tully SE; Cravatt BF Proteome-wide mapping of cholesterol-interacting proteins in mammalian cells. Nat. Methods 2013, 10, 259. [PubMed: 23396283]

(41). Sarkar S; Libby EA; Pidgeon SE; Dworkin J; Pires MM In Vivo Probe of Lipid II-Interacting Proteins. Angew. Chem., Int. Ed 2016, 55, 8401–8404.

(42). Foley HN; Stewart JA; Kavunja HW; Rundell SR; Swarts BM Bioorthogonal chemical reporters for selective in situ probing of mycomembrane components in mycobacteria. Angew. Chem., Int. Ed 2016, 55, 2053–2057.

(43). Kavunja HW; Piligian BF; Fiolek TJ; Foley HN; Nathan TO; Swarts BM A chemical reporter strategy for detecting and identifying O-mycoloylated proteins in Corynebacterium. Chem. Commun 2016, 52, 13795–13798.

(44). Fiolek TJ; Banahene N; Kavunja HW; Holmes NJ; Rylski AK; Pohane AA; Siegrist MS; Swarts BM Engineering the Mycomembrane of Live Mycobacteria with an Expanded Set of Trehalose Monomycolate Analogues. ChemBioChem 2019, 20, 1282–1291. [PubMed: 30589191]

(45). Hanessian S; Lavallee P Synthesis of 6-amino-6-deoxy-α,α-trehalose. Positional isomer of trehalosamine. J. Antibiot 1972, 25, 683–684.

(46). Swarts BM; Holsclaw CM; Jewett JC; Alber M; Fox DM; Siegrist MS; Leary JA; Kalscheuer R; Bertozzi CR Probing the mycobacterial trehalome with bioorthogonal chemistry. J. Am. Chem. Soc 2012, 134, 16123–16126. [PubMed: 22978752]

(47). Sarpe VA; Kulkarni SS Synthesis of Maradolipid. J. Org. Chem 2011, 76, 6866–6870. [PubMed: 21739985]

(48). Stewart JA; Piligian BF; Rundell SR; Swarts BM A Trifunctional Cyclooctyne for Modifying Azide-Labeled Biomolecules with Photocrosslinking and Affinity Tags. Chem. Commun 2015, 51, 17600–17603.

(49). Kuru E; Hughes HV; Brown PJ; Hall E; Tekkam S; Cava F; de Pedro MA; Brun YV; VanNieuwenhze MS In situ Probing of Newly Synthesized Peptidoglycan in Live Bacteria with Fluorescent D-Amino Acids. Angew. Chem., Int. Ed 2012, 51, 12519–12523.

(50). Melzer ES; Sein CE; Chambers JJ; Siegrist MS DivIVA concentrates mycobacterial cell envelope assembly for initiation and stabilization of polar growth. Cytoskeleton 2018, 75, 498–507. [PubMed: 30160378]

(51). García-Heredia A; Pohane AA; Melzer ES; Carr CR; Fiolek TJ; Rundell SR; Chuin Lim H; Wagner JC; Morita YS; Swarts BM; Siegrist MS Peptidoglycan precursor synthesis along the sidewall of pole-growing mycobacteria. eLife 2018, 7, No. e37243. [PubMed: 30198841]

(52). Favrot L; Grzegorzewicz AE; Lajiness DH; Marvin RK; Boucau J; Isailovic D; Jackson M; Ronning DR Mechanism of inhibition of *Mycobacterium tuberculosis* antigen 85 by ebselen. Nat. Commun 2013, 4, 2748. [PubMed: 24193546]

(53). Kamariza M; Shieh P; Ealand CS; Peters JS; Chu B; Rodriguez-Rivera FP; Babu Sait MR; Treuren WV; Martinson N; Kalscheuer R; Kana BD; Bertozzi CR Rapid detection of *Mycobacterium tuberculosis* in sputum with a solvatochromic trehalose probe. Sci. Transl. Med 2018, 10, No. eaam6310.

(54). Siegrist MS; Whiteside S; Jewett JC; Aditham A; Cava F; Bertozzi CR d-Amino Acid Chemical Reporters Reveal Peptidoglycan Dynamics of an Intracellular Pathogen. ACS Chem. Biol 2013, 8, 500–505. [PubMed: 23240806]

(55). Lea-Smith DJ; Pyke JS; Tull D; McConville MJ; Coppel RL; Crellin PK The reductase that catalyzes mycolic motif synthesis is required for efficient attachment of mycolic acids to arabinogalactan. J. Biol. Chem 2007, 282, 11000–11008. [PubMed: 17308303]

(56). Bhatt A; Brown AK; Singh A; Minnikin DE; Besra GS Loss of a mycobacterial gene encoding a reductase leads to an altered cell wall containing beta-oxo-mycolic acid analogs and accumulation of ketones. Chem. Biol 2008, 15, 930–939. [PubMed: 18804030]

(57). Ojha AK; Trivelli X; Guerardel Y; Kremer L; Hatfull GF Enzymatic hydrolysis of trehalose dimycolate releases free mycolic acids during mycobacterial growth in biofilms. J. Biol. Chem 2010, 285, 17380–17389. [PubMed: 20375425]

(58). Yang Y; Kulka K; Montelaro RC; Reinhart TA; Sissons J; Aderem A; Ojha AK A Hydrolase of Trehalose Dimycolate Induces Nutrient Influx and Stress Sensitivity to Balance Intracellular Growth of *Mycobacterium tuberculosis*. Cell Host Microbe 2014, 15, 153–163. [PubMed: 24528862]

(59). Holmes NJ; Kavunja HW; Yang Y; Vannest BD; Ramsey CN; Gepford DM; Banahene N; Poston AW; Piligian BF; Ronning DR; Ojha AK; Swarts BM A FRET-Based Fluorogenic Trehalose Dimycolate Analogue for Probing Mycomembrane-Remodeling Enzymes of Mycobacteria. ACS Omega 2019, 4, 4348–4359. [PubMed: 30842987]

(60). Joshi SA; Ball DA; Sun MG; Carlsson F; Watkins BY; Aggarwal N; McCracken JM; Huynh KK; Brown EJ EccA1, a component of the Mycobacterium marinum ESX-1 protein virulence factor secretion pathway, regulates mycolic acid lipid synthesis. Chem. Biol 2012, 19, 372–380. [PubMed: 22444592]

(61). Lee J-S; Son JW; Jung S-B; Kwon Y-M; Yang C-S; Oh J-H; Song C-H; Kim H-J; Park J-K; Paik T-H; Jo E-K Ex vivo responses for interferon-gamma and proinflammatory cytokine secretion to low-molecular-weight antigen MTB12 of *Mycobacterium tuberculosis* during human tuberculosis. Scand. J. Immunol 2006, 64, 145–154. [PubMed: 16867160]

(62). Wang Q; Liu S; Tang Y; Liu Q; Yao Y MPT64 protein from *Mycobacterium tuberculosis* inhibits apoptosis of macrophages through NF-kB-miRNA21-Bcl-2 pathway. PLoS One 2014, 9, e100949–e100949a. [PubMed: 25000291]

(63). Pethe K; Alonso S; Biet F; Delogu G; Brennan MJ; Locht C; Menozzi FD The heparin-binding haemagglutinin of M. tuberculosis is required for extrapulmonary dissemination. Nature 2001, 412, 190–194. [PubMed: 11449276]

(64). DeJesus MA; Gerrick ER; Xu W; Park SW; Long JE; Boutte CC; Rubin EJ; Schnappinger D; Ehrt S; Fortune SM; Sassetti CM; Ioerger TR Comprehensive Essentiality Analysis of the *Mycobacterium tuberculosis* Genome via Saturating Transposon Mutagenesis. mBio 2017, 8, e02133–16. [PubMed: 28096490]

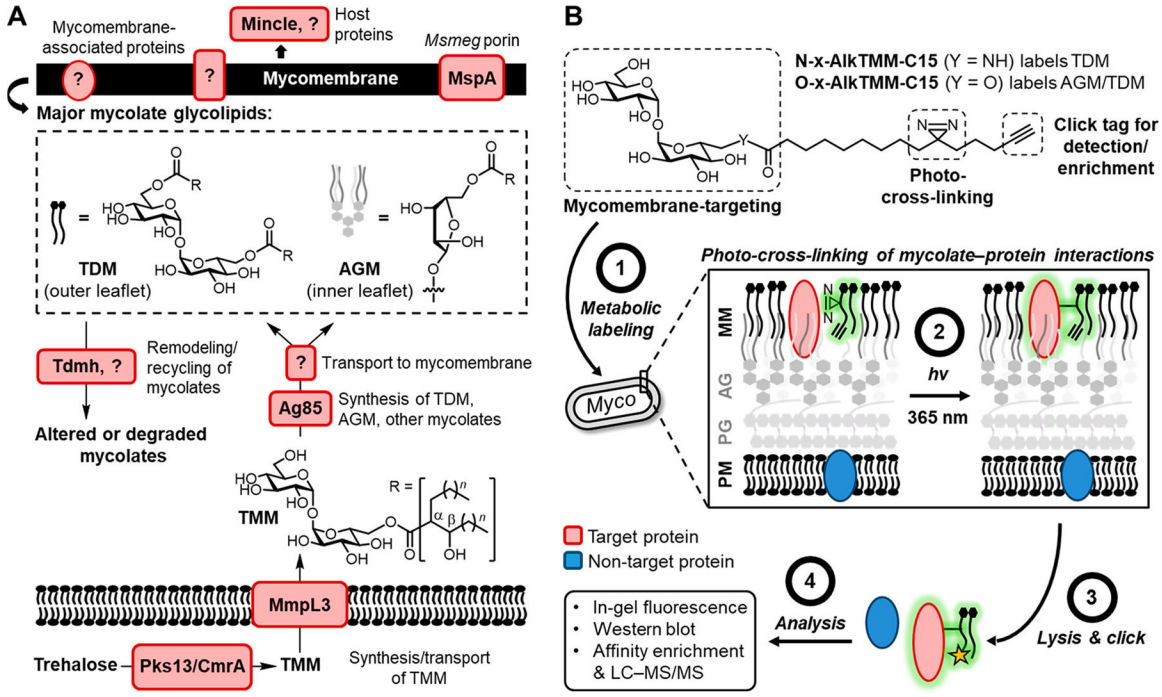

Figure 1.

(A) Metabolism and host interactions of mycolate glycolipids. (B) Strategy for *in vivo* capture and analysis of mycolate-interacting proteins using photoactivatable probes (see Scheme S1 and Supporting Information Discussion).

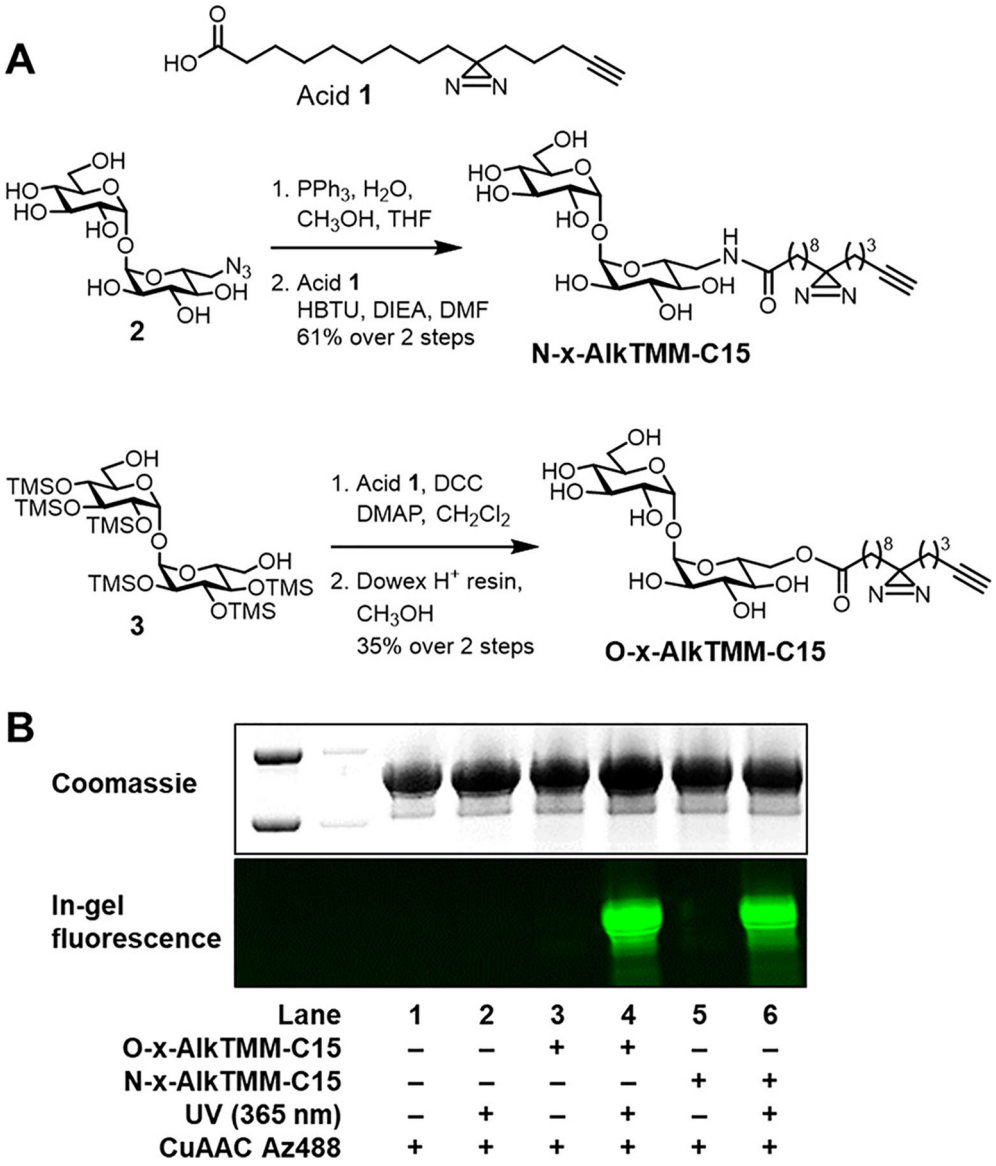

Figure 2.

(A) Syntheses of N- and O-x-AlkTMM-C15. (B) UV-dependent photo-cross-linking of BSA with probes followed by CuAAC-mediated product detection.

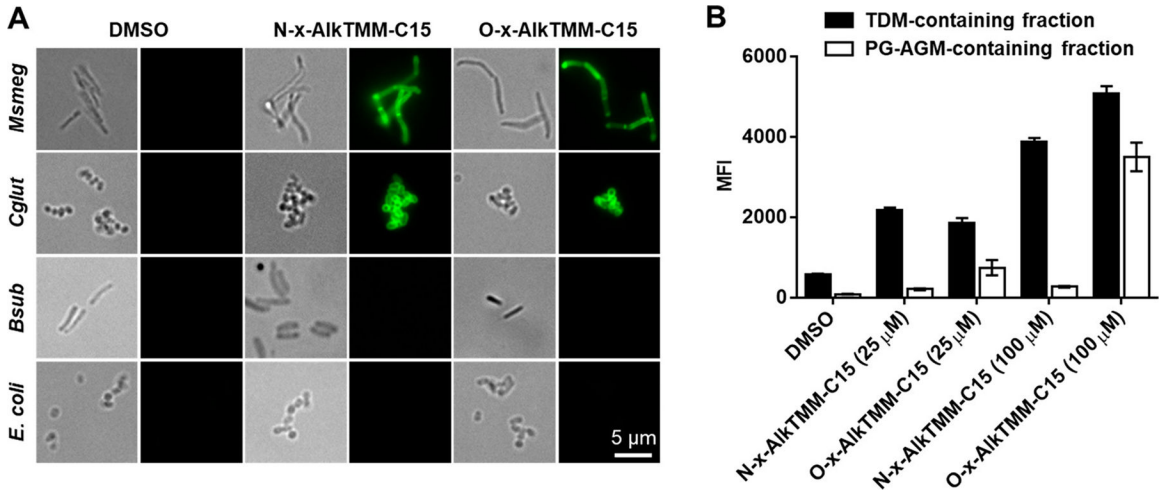

Figure 3.

Mycomembrane labeling with N- and O-x-AlkTMM-C15. (A) Bacteria were cultured in probe (25 μM), reacted with azido-488 by CuAAC, and analyzed by microscopy (Figure S4, flow cytometry). (B) Probe-treated *Msmeg* was reacted with azido-488 by CuAAC and fractionated into PG-AGM- and TDM-containing fractions, and fluorescence was measured. Error bars denote the standard deviation of three replicates. MFI, mean fluorescence intensity in arbitrary units.

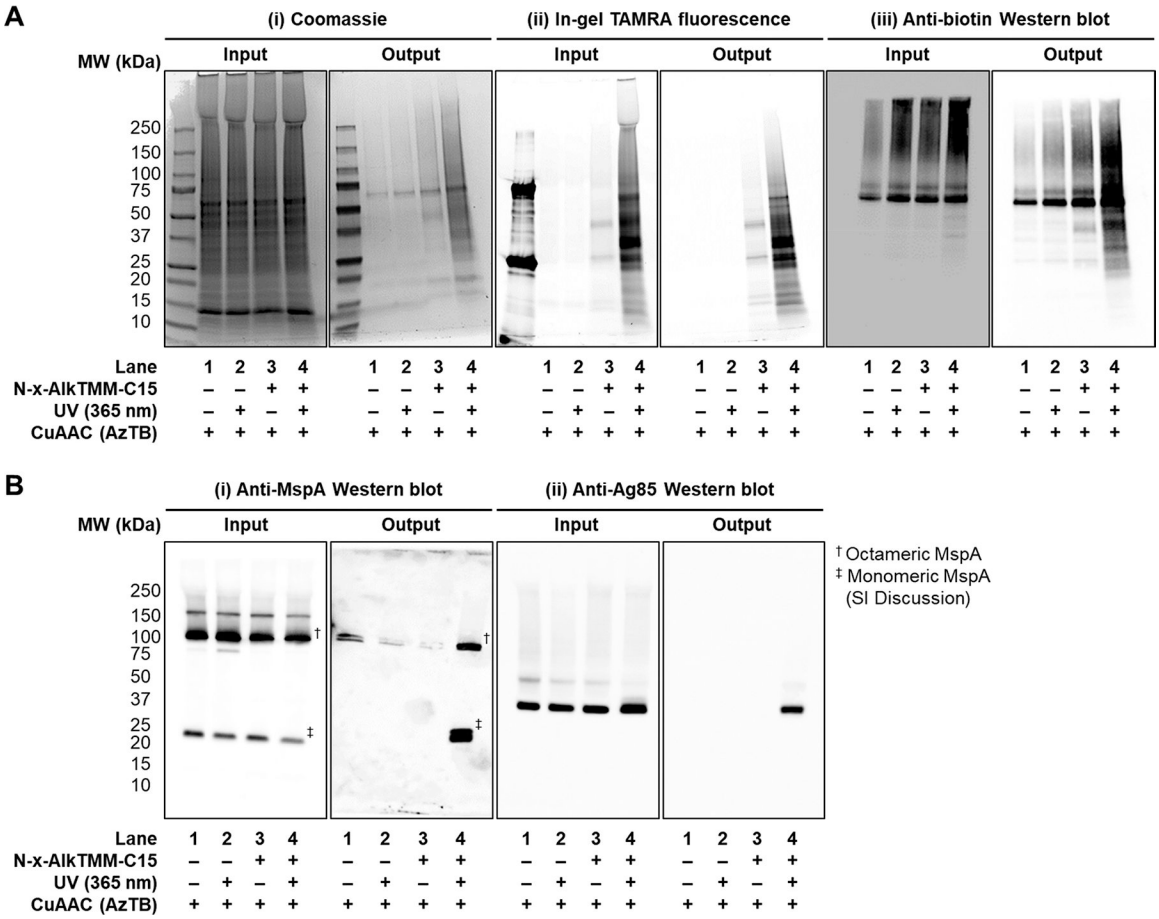

Figure 4.

N-x-AlkTMM-C15-mediated affinity enrichment of mycolate-interacting proteins. *Msmeg* was cultured in N-x-AlkTMM-C15 (100 μM), UV-irradiated, and lysed. Lysates were reacted with AzTB by CuAAC and then analyzed using the indicated method before (input) and after (output) incubation with avidin beads to evaluate enrichment of (A) proteins in general and (B) MspA and Ag85. Data are representative of three independent experiments.

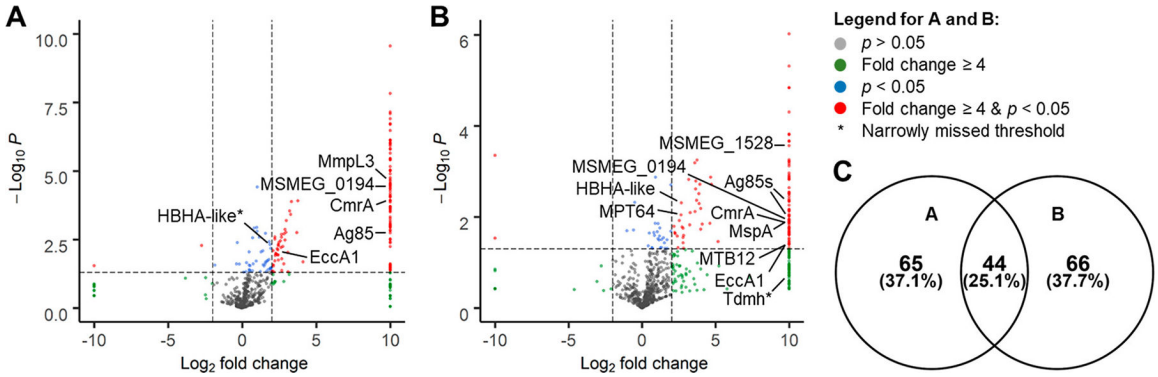

Figure 5.

Volcano plots showing proteins in red that were significantly enriched in N-x-AlkTMM-C15-treated, UV-exposed (+probe+UV) versus nonirradiated (+probe−UV) *Msmeg* grown to OD_{600} (A) ~1.2 or (B) ~4 using click-mediated protein affinity enrichment, tryptic digestion, and LC−MS/MS analysis. Selected proteins of interest are indicated. (C) Venn diagram of proteins enriched in (A) and (B).